PHYSICAL REVIEW B **81**, 060414(R) (2010)

Finite-size effects and magnetic order in the spin-$\frac{1}{2}$ honeycomb-lattice compound $InCu_{2/3}V_{1/3}O_3$

M. Yehia,[1] E. Vavilova,[1,2] A. Möller,[3,4] T. Taetz,[4] U. Löw,[5] R. Klingeler,[1] V. Kataev,[1,*] and B. Büchner[1]
[1]*Leibniz Institute for Solid State and Materials Research IFW Dresden, P.O. Box 270116, D-01171 Dresden, Germany*
[2]*Zavoisky Physical Technical Institute of the Russian Academy of Sciences, 420029 Kazan, Russia*
[3]*Department of Chemistry and Texas Center for Superconductivity, University of Houston, Houston, Texas 77204, USA*
[4]*Institut für Anorganische Chemie, Universität zu Köln, 50939 Köln, Germany*
[5]*Technische Universität Dortmund, Theoretische Physik I, 44221 Dortmund, Germany*

(Received 22 December 2009; revised manuscript received 5 February 2010; published 24 February 2010)

High-field electron spin resonance, nuclear magnetic resonance, and magnetization studies addressing the ground state of the quasi-two-dimensional spin-$\frac{1}{2}$ honeycomb lattice compound $InCu_{2/3}V_{1/3}O_3$ are reported. Uncorrelated finite-size structural domains occurring in the honeycomb planes are expected to inhibit long-range magnetic order. Surprisingly, ESR data reveal the development of two collinear antiferromagnetic (AFM) sublattices below ~20 K, whereas NMR results show the presence of the staggered internal field. Magnetization data evidence a spin reorientation transition at ~5.7 T. Quantum Monte Carlo calculations show that switching on the coupling between the honeycomb spin planes in a finite-size cluster yields a Néel-like AFM spin structure with a substantial staggered magnetization at finite temperatures. This may explain the occurrence of a robust AFM state in $InCu_{2/3}V_{1/3}O_3$ despite an unfavorable effect of structural disorder.

DOI: 10.1103/PhysRevB.81.060414 PACS number(s): 75.50.Ee, 76.30.Fc, 76.60.−k, 75.10.Jm

In planar honeycomb lattice systems a combination of nontrivial topology, strong electronic, spin and orbital correlations, and degeneracies yields a rich variety of ground states, excitations and exotic behaviors that currently attract much attention. The recently discovered exciting phenomena range, e.g., from the quantum Hall effect in graphene,[1,2] superconductivity in MgB_2,[3] and intercalated graphite,[4] to topologically driven quantum phase transitions in anyonic quantum liquids.[5]

Regarding the spin degrees of freedom, an important feature of low-dimensional spin systems is the presence of quantum fluctuations that inhibit long-range order of the quantum spin-$\frac{1}{2}$ lattice. Such an effect essentially depends on the spin coordination number z. The one-dimensional (1D) Heisenberg antiferromagnetic (AFM) $S=1/2$ chain with $z=2$ does not show any magnetic order even at zero temperature,[6] whereas long-range order is possible at $T=0$ in the 2D case[7] as, e.g., in the prominent $S=1/2$ Heisenberg square lattice model with $z=4$. The honeycomb lattice has the minimum possible coordination number of any regular 2D lattice $z=3$. Thus quantum fluctuations there are weaker than in the 1D case but stronger than in the 2D square lattice. Hence, the AFM order for the honeycomb lattice is fragile.[8,9]

Experimentally, low-D spin systems described by the Heisenberg Hamiltonian $\mathcal{H}=2J_{\mathrm{afm}}\Sigma S_i S_j$ are often realized in structurally three dimensional organic- or transition-metal oxide (TMO) compounds where strong AFM exchange interaction J_{afm} between unpaired localized spins occurs along only one or two spacial directions. Owing to residual small three-dimensional (3D) exchange couplings such materials usually exhibit a long-range Néel order at a finite temperature T_N, though, unlike in the 3D magnets, the ordering occurs at much smaller temperatures $T_N \ll J_{\mathrm{afm}}/k_B$.

Recently, a complex TMO compound, $InCu_{2/3}V_{1/3}O_3$, was suggested as a possible candidate for the realization of the $S=1/2$ honeycomb lattice.[10] In its layered hexagonal structure the Cu^{2+} $(3d^9, S=1/2)$ ions are proposed to be arranged in a 2D network of hexagons with the nonmagnetic V^{5+} $(3d^0)$ ions in the center of each hexagon. The honeycomb layers are separated by sheets of $[InO_6]$ polyhedra along the hexagonal c axis. The analysis of the static susceptibility $\chi(T)$ has yielded the exchange parameter $J_{\mathrm{afm}} \simeq 140$ K of the honeycomb spin lattice.[10] A later structural neutron diffraction study revealed that a structural $^2_\infty\{V_1Cu_{6/3}\}$ order in the hexagonal planes has a finite correlation length $\xi_{\mathrm{st}} \sim 300$ Å and that these structural domains are randomly arranged along the c axis.[11] As has been argued in Ref. 11 this structural disorder rendering finite values of the spin-spin correlation length $\xi_s \leq \xi_{\mathrm{st}}$ concomitant with the substantial spacing between the honeycomb planes and with the low spin coordination number in the planes could preclude a 3D Néel order in $InCu_{2/3}V_{1/3}O_3$. Thus the kinklike anomalies in $\chi(T)$ dependence at 30 and 38 K previously identified with the transition to the long-range ordered state[10] have been tentatively assigned to glasslike order of unsaturated spins in domain boundaries.[11]

To obtain insights into the nature of the ground state of $InCu_{2/3}V_{1/3}O_3$, we have investigated its magnetic properties using two local spin probe techniques, high-field electron spin resonance (ESR), and nuclear magnetic resonance (NMR). These experiments were complemented by measurements of the field dependence of the static magnetization $M(B)$ and by quantum Monte Carlo calculations. From ESR and NMR data we have obtained evidence for the development of the AFM sublattices in the spin system below ~20 K which according to the $M(B)$ data experience a reorientation transition at a field of ~5.7 T. Our Monte Carlo calculations reveal that switching on the interlayer coupling in a finite-size honeycomb spin domain yields the formation of the staggered sublattices with substantial sublattice magnetization at a finite temperature. We conclude that structural disorder does not inhibit the Néel ordered state in $InCu_{2/3}V_{1/3}O_3$ at least on a spacial scale of structural domains which, owing to their large size, has properties very

similar to the long-range AFM order in the infinite systems.

Clean stoichiometric powder of $InCu_{2/3}V_{1/3}O_3$ was synthesized and thoroughly characterized as described in Ref. 11. From it we prepared an "oriented" sample by mixing the powder with epoxy and letting it harden in a magnetic field of 1 T. Owing to the specific anisotropy of the Cu^{2+} g factor[10] the c axis of the powder particles was oriented perpendicular to the orientation axis (hereafter o axis) defined by the direction of the applied field, as confirmed by x-ray diffraction experiments. ESR was measured with a home made spectrometer on the basis of the millimeter wave-vector network analyzer from AB Millimeter, Paris, combined with a 17 T superconducting magnetocryostat from Oxford Instruments Ltd.[12] NMR data were collected on a Tecmag pulse solid-state NMR spectrometer with a 9.2 T superconducting magnet from Magnex Scientific. The NMR spectra were obtained by measuring the intensity of the Hahn echo versus magnetic field. The T_1 relaxation time was measured with the method of stimulated echo. Static magnetization was measured with a superconducting quantum interference device magnetometer from Quantum Design. In all experiments the magnetic field was applied parallel to the o axis, i.e., perpendicular to the hexagonal c axis.

In the previous ESR experiment performed at a standard X-band "low" frequency $\nu=9.47$ GHz a strong paramagnetic Cu^{2+} resonance signal clearly visible at high temperatures experienced at $T<80$ K strong broadening and shift and could not be detected below 50 K.[10] Since such a behavior could be indicative of an opening of the energy gap for resonance excitations, e.g., due to the establishment of the AFM order, we have measured in the present work the ESR spectra at low T in a broad frequency domain extending into the sub-THz range.

ESR spectra at various frequencies ν collected at $T=8$ K for a magnetic field applied parallel to the orientation axis ($B\|o$ axis) are shown in Fig. 1(a). Several resonance modes are visible. At high frequencies three modes can be detected, L_1, L_2, and L_3. They shift toward higher fields by increasing the ν. At lower frequencies, the L_4 mode can be observed which, in contrast, moves toward lower fields by increasing the ν. The evolution of L_1-L_4 is summarized in the frequency-field (ν vs B) diagram in Fig. 1(b). Notably, none of the $\nu(B)_{Li}$ branches correspond to a paramagnetic resonance condition $h\nu=g\mu_B B_{res}$. Here h is the Planck constant and μ_B is the Bohr magneton. Modes L_1, L_3, and L_4 are obviously gapped. Extrapolation of L_3 and L_4 branches to zero field yields an estimate of the gap value $\Delta\simeq 190$ GHz. Mode L_4 softens with increasing the field strength revealing a critical field $B_c\sim 5.5-6$ T where $\nu_{L4}\to 0$. Above B_c mode L_2 emerges. In fact, taking the above estimate of Δ and the value of the g factor for $B\|o$ axis $g=2.23$ obtained from the X-band measurements at high T (not shown) it is possible to reasonably model the L_1-L_4 branches with the AFM resonance (AFMR) relations for a uniaxial two-sublattice antiferromagnet.[13] L_3 and L_4 can be represented as $h\nu=\Delta\pm g\mu_B B_{res}$, where the plus and minus signs correspond to L_3 and L_4, respectively. L_2 that appears above B_c can be described as $h\nu/g\mu_B=\sqrt{B_{res}^2-\Delta^2}$. Finally, L_1 follows the relation $h\nu/g\mu_B=\sqrt{\Delta^2+B_{res}^2}$. Apart from some systematic discrepancy for the L_2 branch the model agrees

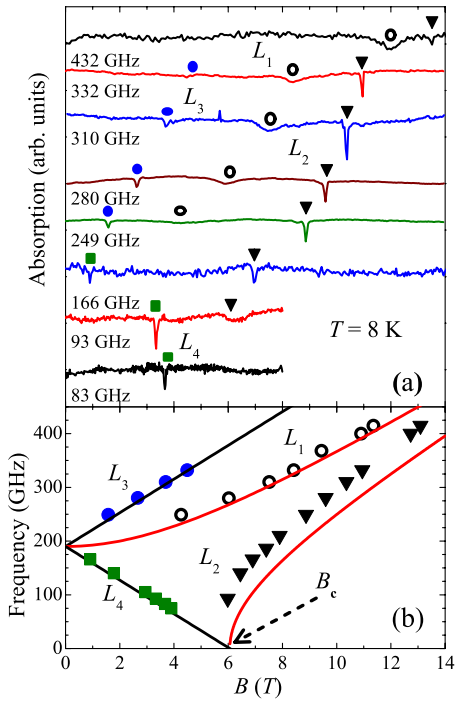

FIG. 1. (Color online) Frequency ν dependence of the ESR signals at $T=8$ K: (a) selected spectra at different ν. Open circles, solid circles, triangles and squares indicate the resonance field B_{res} of the lines L_1-L_4; (b) the ν vs B diagram of the resonance modes. The symbols correspond to respective L_i in panel (a), solid lines are model curves (see the text).

well with the experiment. The behavior of L_2, L_3, and L_4 is typical for the situation when a magnetic field is applied parallel to some "easy" axis of an antiferromagnet, whereas L_1 corresponds to a "hard" direction.[13] The field B_c at which for L_2 and L_4 the frequency $\nu\to 0$ is the spin-flop field B_c related to Δ as $B_c=(h/g\mu_B)\Delta$.[13] Taking $\Delta\simeq 190$ GHz one obtains $B_c\sim 6$ T. Since B was applied in the honeycomb plane of $InCu_{2/3}V_{1/3}O_3$, there must be therefore some easy direction in the plane that defines the AFM vector of two sublattices. Obviously the direction of this in-plane easy axis of each powder particle is random in the sample, because specific in-plane crystallographic directions in our sample are not defined. Therefore both easy and hard AFMR modes are present. We note that these modes can be seen at temperatures up to ~ 20 K.

Further evidence for the occurrence of the AFM sublattices and related staggered magnetization has been obtained from the NMR measurements of ^{51}V ($I=7/2$) and ^{114}In ($I=9/2$) nuclei in $InCu_{2/3}V_{1/3}O_3$. At high temperatures the spectra of both nuclei consist of a main line and a typical satellite structure arising due to the quadrupole interaction. In is positioned outside the hexagonal (Cu,V)-plane asymmetrically with respect to the Cu honeycomb ring. Hence one could expect at low T an uncompensated staggered field at this position. Indeed, below 20 K, where AFMR modes are observed in the ESR experiment, the ^{114}In NMR signal experiences a remarkable change if measured in a magnetic field B_{NMR} smaller than B_c [cf. Figs. 2(a) and 2(b)]. At $T=35$ K the line is unsplit regardless the field of the mea-

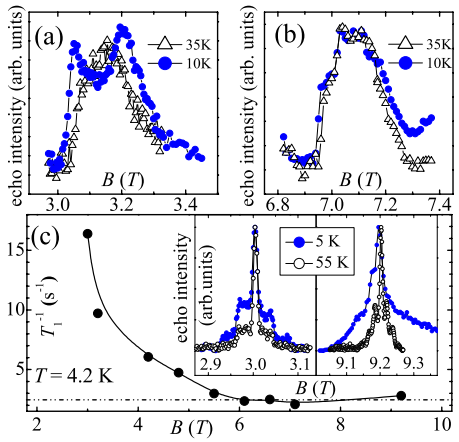

FIG. 2. (Color online) ^{114}In NMR line at 35 and 10 K at fields (a) smaller and (b) larger than $B_c \sim 6$ T; (c) T_1^{-1} relaxation rate of ^{51}V nuclei as a function of B at $T=4.2$ K. Lines are guides for the eye. Inset: ^{51}V NMR spectra at fields smaller (left) and larger (right) than B_c at 55 and 5 K.

surement. However, at $T=10$ K the signal splits in two components for $B_{NMR}<B_c$, whereas it remains unsplit for $B_{NMR}>B_c$. This observation strongly supports the scenario of compensated collinear AFM sublattices at $B<B_c$ which turn into the spin-flop state at $B>B_c$. The ^{51}V NMR data agree with this scenario. The V site is symmetric with respect to the Cu sites. Therefore the staggered fields from the honeycomb spin lattice should be compensated at this position. In fact, the ^{51}V NMR spectrum does not change qualitatively with decreasing the T at $B_{NMR}<B_c$ and shows the presence of a broad background at a high field [Fig. 2(c), inset]. The absence of the broadening of the main line suggests that this background is due to the influence of structural domain walls where uncompensated spins create a distribution of the local magnetic fields. Remarkably, though the ^{51}V NMR signal remains unsplit at low T, the ^{51}V longitudinal nuclear relaxation rate T_1^{-1} shows a substantial field dependence: It decreases by a factor of seven by approaching the B_c and shows no field dependence at $B_{NMR}>B_c$ [Fig. 2(c)]. An initial rapid drop of T_1^{-1} at $B \sim 3$ T could be due to a field suppression of magnetic fluctuations caused by impurity freelike spins. However, according to the magnetization measurements (see Fig. 3 and its discussion below) these spins are fully polarized at stronger fields. Thus a further substantial reduction in T_1^{-1} is likely to be related with the approach to the critical field B_c. The sensitivity of T_1^{-1} to the spin structure may be related to magnetic anisotropy that defines a specific easy orientation in the honeycomb spin plane and possibly produces a small uncompensated fluctuating field at the V nuclei in the collinear phase that become ineffective for the T_1 relaxation after the spin reorientation has occurred.

Motivated by the findings of the local ESR and NMR techniques we have performed the magnetization measurements on an oriented powder sample of $InCu_{2/3}V_{1/3}O_3$ for a magnetic field applied parallel to the o axis. The temperature dependence of the magnetic susceptibility $\chi=M/B$ at $B=1$ T demonstrates the same behavior as observed before in Ref. 11 (not shown). The field dependence of the magnetization $M(B)$ at different T is presented in Fig. 3. The curvature of the $M(B)$ at low fields is likely due to a small amount of freelike spins, which also yield a Curie-like tail in the T dependence of χ (Ref. 11). The $M(B)$ dependence at the lowest temperature $T=2$ K exhibits a pronounced steplike increase in M at $B \simeq 5.7$ T. It can be straightforwardly interpreted as a critical field B_c for the spin reorientation, in a nice agreement with ESR and NMR data. By increasing the T the step continuously broadens, slightly shifts toward higher fields and finally smoothly vanishes above $\sim$20 K [Fig. 3, insets (a,b)].

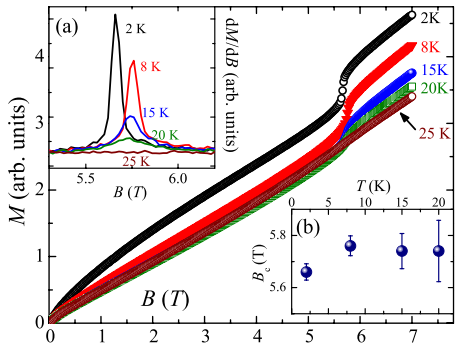

FIG. 3. (Color online) Field dependence of the magnetization $M(B)$ at different temperatures for $B\|$ o-axis after a subtraction of a small T-independent spurious ferromagneticlike signal persisting up to room temperature. Inset: (a) field derivative of $M(B)$; (b) T dependence of the reorientation field. Error bars correspond to the width of the transition.

Thus the results of three different techniques strongly suggest the formation of collinear AFM Néel sublattices in the $S=1/2$ honeycomb plane in $InCu_{2/3}V_{1/3}O_3$ at a finite temperature. As discussed in Ref. 11 the absence of the magnetic anomaly in the specific heat C_p does not exclude the occurrence of the magnetic phase transition in a low-dimensional system such as $InCu_{2/3}V_{1/3}O_3$ due to residual interactions in the third dimension. If the ordering temperature T_N is substantially smaller than J_{afm}/k_B, most of the magnetic entropy S_{mag} is already gone at $T \sim J_{afm}/k_B$ due to the 2D in-plane AFM correlations. Thus an additional change in S_{mag} at T_N might be small and not visible in the C_p owing to a substantial phononic background. The question arises if this 3D situation is realized in $InCu_{2/3}V_{1/3}O_3$ despite the occurrence of disordered finite-size structural domains. To address this issue we have performed a computational study of a finite-size spin-$\frac{1}{2}$ clusters on the honeycomb lattice by means of a continuous Euclidean time quantum Monte Carlo algorithm that includes the coupling in the third dimension.[14] We find that the Néel-type structure and the staggered magnetization m_{st}, otherwise present in the 2D case only at $T=0$, develops in a rather narrow interval at a finite temperature that depends on the strength of the interlayer coupling J_z. As shown in the main panel of Fig. 4 a temperature interval where $m_{st}(T)$ exhibits a steplike increase is mainly determined by the value of J_z whereas the sharpness of this step increases with the increase in the cluster size (inset of Fig. 4). Note that in $InCu_{2/3}V_{1/3}O_3$ the size of in-plane structural domains amounts to $\sim$300 Å (Ref. 11) which corresponds to $\sim 90 \times 90$ spin sites, i.e., a much larger number than in our

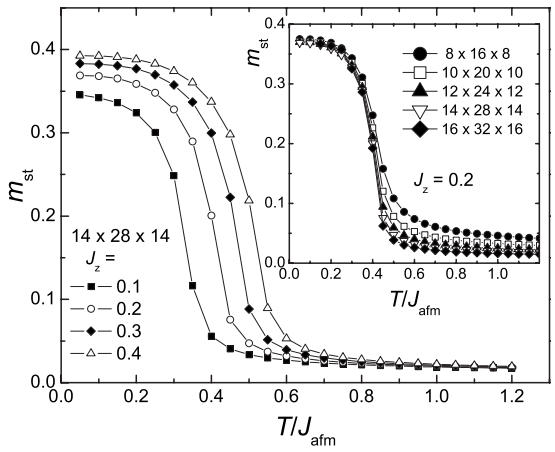

FIG. 4. T dependence of the staggered magnetization m_{st} of the honeycomb lattice with interplane couplings J_z=0.1, 0.2, 0.3 and $0.4J_{afm}$ for the system size $14\times28\times14$. Inset: m_{st} vs T/J_{afm} for $J_z=0.2J_{afm}$ for different system sizes.

model calculation. Thus one should expect quite a sharp setup of the two-sublattice collinear AFM Néel spin structure and the occurrence of the staggered magnetization in $InCu_{2/3}V_{1/3}O_3$ that experimentally would be difficult to discriminate from a true magnetic phase transition expected in the thermodynamic limit. Finally, regarding modeling of the finite-size systems, we mention here that a calculation in the framework of the (anisotropic) Heisenberg model of the ESR response of the AFM cluster comprising eight spins only already yields AFMR modes of a substantial intensity that for the easy axis direction have qualitatively similar properties as those shown in Fig. 1.[15]

In summary, by studying ESR, NMR and static magnetization of the oriented powder sample of the honeycomb spin-$\frac{1}{2}$ lattice compound $InCu_{2/3}V_{1/3}O_3$, we have found strong experimental evidence for the formation of the Néel-type collinear AFM spin structure at temperatures below $\sim$20 K and a respective development of the staggered magnetization. A reorientation of spin sublattices in a field of $\sim$5.7 T has been clearly identified in the magnetization and magnetic resonance data. The AFM ordering of spins in $InCu_{2/3}V_{1/3}O_3$ takes place despite the low spin coordination number, the pronounced structural two dimensionality as well as the presence of the finite-size incoherent structural domains. Our experimental results are corroborated by the quantum Monte Carlo study of the finite-size honeycomb spin layers coupled in the third dimension. It reveals a sharp development of the staggered magnetization at a finite temperature that in the thermodynamic limit would correspond to a phase transition to the AFM long-range ordered state.

The work was supported in part by the German-Russian cooperation project of the DFG (Grant No. 436 RUS 113/936/0-1) and by the Russian Foundation for Basic Research (Grant No. 08-02-91952-NNIO-a). M.Y. acknowledges the DAAD for a scholarship, and T.T. acknowledges the DFG (SFB608) for support.

*v.kataev@ifw-dresden.de

[1] K. S. Novoselov, A. K. Geim, S. V. Morozov, D. Jiang, M. I. Katsnelson, I. V. Grigorieva, S. V. Dubonos, and A. Firsov, Nature (London) **438**, 197 (2005); Y. Zhang, Y.-W. Tan, H. L. Stormer, and P. Kim, *ibid.* **438**, 201 (2005).

[2] X. Du, I. Skachko, F. Duerr, A. Luican, and E. Y. Andrei, Nature (London) **462**, 192 (2009); K. I. Bolotin, F. Ghahari, M. D. Shulman, H. L. Stormer, and P. Kim, *ibid.* **462**, 196 (2009).

[3] J. Nagamatsu, N. Nakagawa, T. Muranaka, Y. Zenitani, and J. Akimitsu, Nature (London) **410**, 63 (2001).

[4] J. E. Weller, M. Ellerby, S. S. Saxena, R. P. Smith, and N. T. Skipper, Nat. Phys. **1**, 39 (2005).

[5] C. Gils, S. Trebst, A. Kitaev, A. W. W. Ludwig, M. Troyer, and Z. Wang, Nat. Phys. **5**, 834 (2009).

[6] P. W. Anderson, Phys. Rev. **86**, 694 (1952).

[7] N. D. Mermin and H. Wagner, Phys. Rev. Lett. **17**, 1133 (1966); P. C. Hohenberg, Phys. Rev. **158**, 383 (1967).

[8] R. F. Bishop and J. Rosenfeld, Int. J. Mod. Phys. B **12**, 2371 (1998).

[9] J. B. Fouet, P. Sindzingre, and C. Lhuillier, Eur. Phys. J. B **20**, 241 (2001).

[10] V. Kataev, A. Möller, U. Löw, W. Jung, N. Schittner, M. Kriener, and A. Freimuth, J. Magn. Magn. Mater. **290**, 310 (2005).

[11] A. Möller, U. Löw, T. Taetz, M. Kriener, G. Andre, F. Damay, O. Heyer, M. Braden, and J. A. Mydosh, Phys. Rev. B **78**, 024420 (2008).

[12] C. Golze, A. Alfonsov, R. Klingeler, B. Büchner, V. Kataev, C. Mennerich, H.-H. Klauss, M. Goiran, J.-M. Broto, H. Rakoto, S. Demeshko, G. Leibeling, and F. Meyer, Phys. Rev. B **73**, 224403 (2006).

[13] E. A. Turov, *Physical Properties of Magnetically Ordered Crystals* (Academic, New York, 1965).

[14] U. Löw, Condens. Matter Phys. **12**, 497 (2009).

[15] A. Ogasahara and S. Miyashita, J. Phys. Soc. Jpn. **69**, 4043 (2000).